Available online at www.sciencedirect.com
SCIENCE DIRECT®
Journal of Power Sources 119–121 (2003) 330–337
JOURNAL OF POWER SOURCES
www.elsevier.com/locate/jpowsour

The role of Li-ion battery electrolyte reactivity in performance decline and self-discharge

Steven E. Sloop, John B. Kerr*, Kim Kinoshita

Lawrence Berkeley National Laboratory, MS 62 203 1 Cyclotron Road, Berkeley, CA 94720, USA

Abstract

The purpose of this paper is to report on the reactivity of PF_5 and EC/linear carbonates to understand the thermal and electrochemical decomposition reactions of $LiPF_6$ in carbonate solvents and how these reactions lead to the formation of products that impact the performance of lithium-ion batteries. The behavior of other salts such as $LiBF_4$ and LiTFSI are also examined. Solid $LiPF_6$ is in equilibrium with solid LiF and PF_5 gas. In the bulk electrolyte, the equilibrium can move toward products as PF_5 reacts with the solvents. The Lewis acid property of the PF_5 induces a ring-opening polymerization of the EC that is present in the electrolyte and can lead to PEO-like polymers. The polymerization is endothermic until 170 °C and is driven by CO_2 evolution. Above this temperature the polymerization becomes exothermic and leads to a violent decomposition. The PEO-like polymers also react with the PF_5 to yield further products that may be soluble in the electrolyte or participate in solid electrolyte interphase (SEI) formation in real cells. GPC analysis of the heated electrolytes indicates the presence of material with M_w up to 5000. More details on the polymerization reactions and further reactions with PF_5 are reported. Transesterification and polymer products are observed in the electrolytes of cycled and aged Li-ion cells. Formation of polymer materials which are further cross-linked by reaction with acidic species leads to degradation of the transport properties of the electrolyte in the composite electrodes with the accompanying loss of power and energy density. Generation of CO_2 in lithium-ion cells leads to saturation of the electrolyte and cessation of the polymerization reaction. However, CO_2 is easily reduced at the anode to oxalate, carbonate and CO. The carbonate contributes to the SEI layer while the oxalate is sufficiently soluble to reach the cathode to be re-oxidized to CO_2 thus resulting in a shuttle mechanism that explains reversible self-discharge. Irreversible reduction of CO_2 to carbonate and CO partially accounts for irreversible self-discharge.

Keywords: Lithium-ion batteries; Carbonate electrolyte; Lewis acid salts; Polymerization; CO_2 generation and reduction; Capacity and power fade

1. Introduction

The typical non-aqueous electrolyte for commercial Li-ion cells is a solution of $LiPF_6$ in linear and cyclic carbonates such as dimethyl carbonate and ethylene carbonate, respectively [1,2]. During battery operation, the anion plays an important role in the formation of the solid electrolyte interphase (SEI) layer, and the stability of the Li salt can be crucial. For example, perchlorate or nitrate salts may be explosive when mixed with organic solvents [3]. Hexafluorophosphate (PF_6^-) salts can produce PF_5 gas [4], a strong Lewis acid [5] which can react with the solvent components of the electrolyte. Similar reactions have been observed for $LiAsF_6$ [6]. There is evidence to suggest that $LiPF_6$ solutions in trioxane give cleavage of ether linkages [7]. Studies of liquid electrolytes have addressed the thermal instability of $LiPF_6$ solutions [8], but the role of PF_5 in the reaction with carbonate electrolytes for Li-ion batteries has only recently been evaluated [9]. The purpose of this report is to explore further the reactivity of PF_5 and EC/linear carbonates to understand the thermal and electrochemical decomposition reactions of $LiPF_6$ in carbonate solvents and how these reactions lead to the formation of products that impact the performance of Li-ion batteries. The behavior of other salts such as $LiBF_4$ and LiTFSI is also examined.

2. Experimental

2.1. Thermal decomposition of the $LiPF_6$ electrolyte (thermal reaction)

Solutions of 1 M $LiPF_6$ electrolyte in of EC/DMC or EC/EMC (1:1 mol ratio) were heated at various temperatures in glass vials sealed under a He atmosphere. Vials were removed from heat at regular intervals and the solutions were analyzed by gas chromatography (HP580 Series II GC

* Corresponding author. Tel.: +1-510-486-6279; fax: +1-510-486-4995.
E-mail address: jbkerr@lbl.gov (J.B. Kerr).

0378-7753/03/$ – see front matter © 2003 Elsevier Science B.V. All rights reserved.
doi:10.1016/S0378-7753(03)00149-6

equipped with a cold on-column inlet and a flame ionization detector). Thermogravimetric analysis (TGA, Perkin-Elmer TGA 7) of $LiPF_6$ (reagent grade, Advance Research Chemicals Inc.) was performed using an isothermal method under flowing nitrogen. A sample of salt (20 mg) was loaded in the drybox and transferred under He to the TGA sample holder, the sample was heated to 70 °C, for example, and the weight change was monitored over time. For comparison, TGA was performed on lithium bis(trifluoromethanesulfonyl)imide (LiTFSI, 3 M) and trifluoromethane sulfonate (LiTF, Aldrich). These salts maintained constant weight to over 300 °C in identical experiments to the $LiPF_6$.

2.2. Reaction of EC/DMC and PF_5 (direct reaction)

A Schlenk flask containing 0.25 g of $LiPF_6$ (Research Chemicals, reagent) was heated (100–120 °C) under argon for 30 min to quantitatively produce PF_5 gas. The gas was transferred from the generator flask through a vacuum line to a reaction flask containing 20 ml of solvent. The reaction flask was immersed in liquid nitrogen to solidify the solvents and PF_5. The excess PF_5 was expelled from the vacuum line with flowing argon, and the mixture of PF_5 and EC/DMC was slowly warmed to room temperature before transferring to a helium-filled drybox.

Gas chromatography (GC) was used to analyze the solutions. A typical sample was prepared by dilution of one drop of electrolyte with 10 ml of dichloromethane; alternatively, the sample was quenched with excess water (Burdick & Jackson distilled in glass) and extracted into dichloromethane. The products noted in the GC traces do not appear to change after exposure to water. For the quantitative treatments, an internal standard, diethylene glycol dibutylether (Aldrich), was employed. It was noted that the internal standard also reacted when present in the heated electrolyte solutions which is consistent with the known reactivity of ethers with PF_5. To avoid this, the standard was added to the methylene chloride solution used to extract the aqueous solutions.

Electrolyte solutions and cell components were analyzed by the same extraction process. Cell components such as electrodes or separators were immersed in purified water (Burdick & Jackson, distilled in glass). The water samples were then filtered through a 0.2 μm filter before injection on a HPLC system (Rainin Instruments or Agilent 1100 Series) or Capillary Electrophoresis system (Hewlett-Packard ^{3D}CE). The HPLC system was equipped with a PL Aquagel Mixed 8 Gel Permeation Chromatography column. The eluent was water (1 ml/min flow rate) and the detector was a refractive index detector. The CE system was equipped with an Agilent fused silica capillary with a bubble-cell detection window or high sensitivity cell. The capillary was either bare fused silica or PVA coated. The aqueous extracts were then solvent extracted with methylene chloride containing internal standard and the resulting solutions analyzed by GC or GC/MS (Agilent 6890/5973 MSD).

Cyclic voltammetry and electrochemical testing was carried out with a PAR173 potentiostat with a 273 interface controlled with Corrware software package version 2.1 (Scribner Associates). Electrode components were obtained from 18650 Li-ion cells that had undergone accelerated calendar and cycle life aging [10,11].

3. Results and discussion

Solid $LiPF_6$ is in equilibrium with solid LiF and PF_5 gas. Fig. 1 shows the results of isothermal TGA experiments on

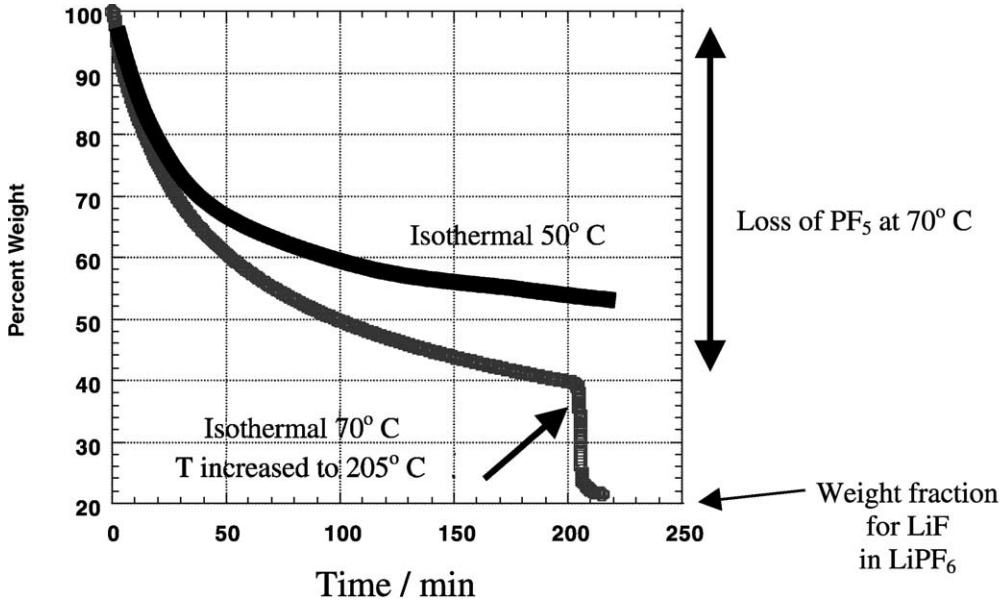

Fig. 1. Isothermal weight loss for $LiPF_6$ in thermogravimetric analysis (TGA) experiments. Dry salt heated in flowing nitrogen.

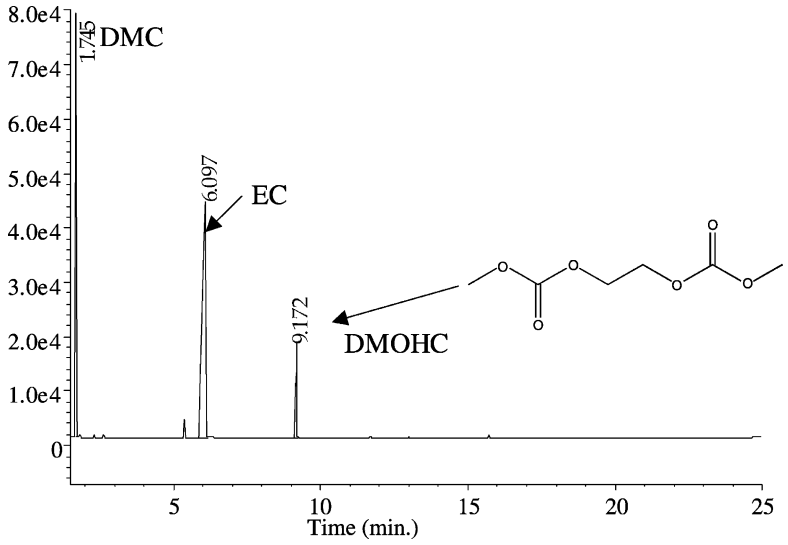

Fig. 2. Gas chromatography trace of heated $LiPF_6$ EC:DMC electrolyte solution. Sample injected at −15 °C using a cold on-column inlet. See Section 2 for column conditions.

solid $LiPF_6$ which demonstrate the equilibrium. The reaction temperature and the pressure of PF_5 gas determine the equilibrium position. Removal of PF_5 gas consumes $LiPF_6$ and produces LiF. For a $LiPF_6$ solution, the analogous equilibrium exists. Because LiF is insoluble, only the concentration of $LiPF_6$ and PF_5 determine the equilibrium position.

$$LiPF_{6\,(sol)} \rightleftharpoons LiF_{(s)} + PF_{5\,(sol)} \quad (1)$$

In electrolyte solutions, the equilibrium can move toward products as PF_5 reacts with the solvents. Fig. 2 shows the gas chromatography analysis of a solution of $LiPF_6$ EC:DMC heated in a glass vial at 85 °C for several hours. A considerable amount of the dimeric compound dimethyl-2,5-dioxahexane carboxylate (DMOHC) is observed in the solution. Close examination of the chromatogram reveals

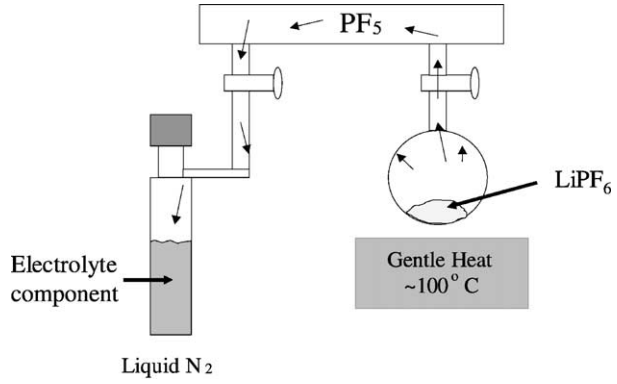

Fig. 3. PF_5 generator and reactor for electrolyte components. Schlenk-line used to create scaled up version of TGA experiment.

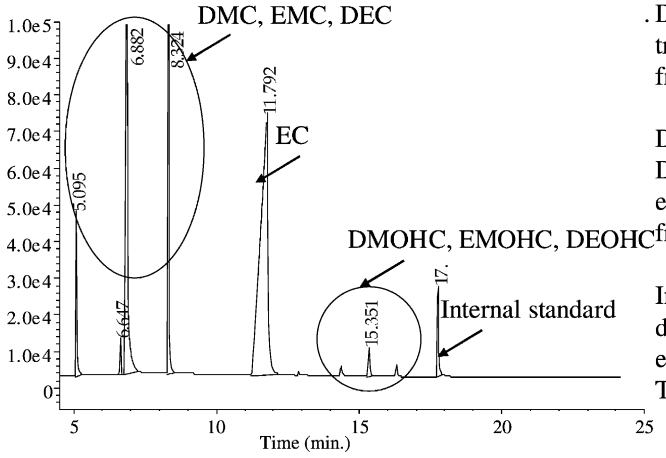

. DMC and DEC are transesterification products from EMC.

DMOHC, EMOHC & DEOHC are mixed trans-esterification products from EC and EMC

Internal standard is diethylene glycol dibutyl ether –a short chain PEO. This also reacts with $LiPF_6$.

Fig. 4. GC analysis of $LiPF_6$ EC:EMC solution heated for 1 day at 85 °C.

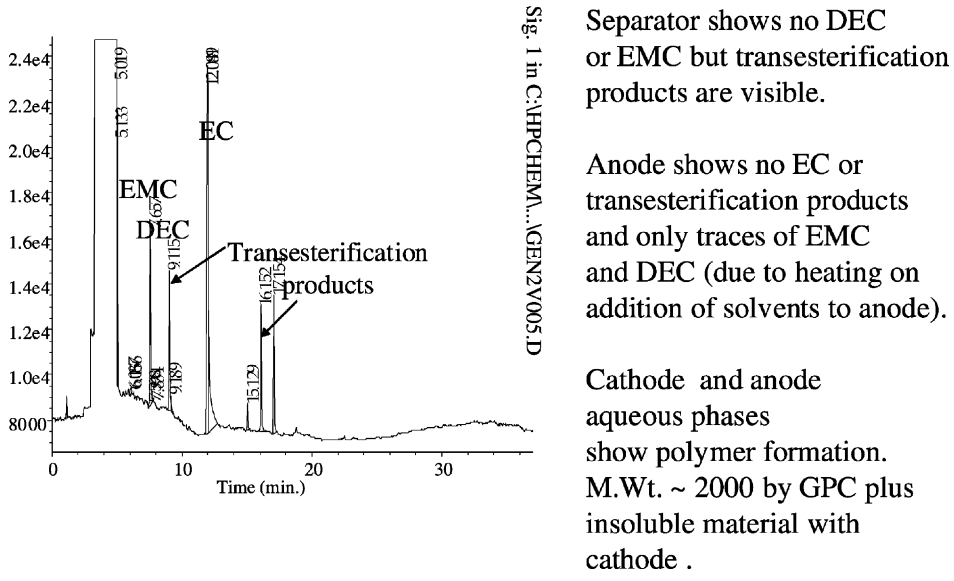

Fig. 5. GC analysis of aqueous extracts of a $LiAl_{0.05}Ni_{0.80}Co_{0.15}O_2$ cathode taken from a virgin 18650 cell (formation cycle only followed by storage at ambient temperatures).

the presence of less volatile products. (Note the GC inlet is a cold, on-column inlet that avoids any thermal reactions upon injection).

The TGA experiment is scaled up and reaction with solvent is simulated by the Schlenk-line experiment shown in Fig. 3. The $LiPF_6$ salt is placed in one vessel where it is heated. The vessel is connected through the vacuum line to a second vessel that contains the electrolyte solvents at liquid N_2 temperature. Upon warming, the solvent mixture turns brown and GC analysis of the resulting mixture gives a similar result to Fig. 2.

Thermal treatment of EC/EMC solutions gives similar results. Fig. 4 shows the GC trace of a heated solution. In this case an internal standard was added to allow quantitative analysis. The standard, diethylene glycol dibutylether, was observed to react in this medium also, indicating that ether solvents are also attacked by PF_5. The standard is added to samples after quenching with water to avoid this problem. The GC trace shows the presence of DMC and DEC, formed by acid-catalyzed transesterification of the linear carbonates, and the presence of DMOHC, EMOHC and DEOHC which are formed by acid-catalyzed transesterification reactions involving EC and the linear EMC.

Fig. 5 shows the results of a gas chromatography analysis of the electrolyte products on a cathode from an 18650 cell that had only undergone the formation cycle and was stored at 25 °C. The similarity of the products with those observed in Fig. 4 is striking. Further analysis of the extracts by GPC

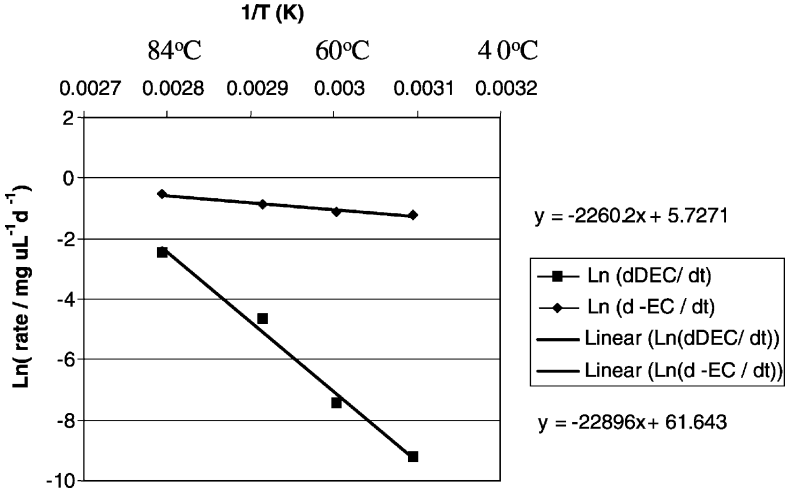

Fig. 6. Arrhenius behavior of DEC and EC reactions with $LiPF_6$ at elevated temperatures. Rate of disappearance of EC and appearance of DEC from heated $LiPF_6$ EC:EMC solution followed as a function of temperature. At 25 °C rate of EC reaction remains high but rate of DEC reaction is negligible and no volatile transesterification products are observed. Transesterification products observed at elevated temperatures account for loss of EMC but EC loss cannot be accounted for by GC analysis of volatile products—indicates formation of non-volatile polymeric material.

using water eluent revealed the presence of higher molecular weight products (>5000) by comparison with PEO standards.

The use of the internal standard shown in Fig. 4 allows quantitative measures of the reactivity of the electrolyte components as the concentration of the components can be followed as a function of the conditions. Fig. 6 shows the results of such measurements as a function of temperature. It can be seen that both linear and cyclic carbonate solvents are reactive in the presence of $LiPF_6$ but the reactivity of EC is much higher, particularly at low temperatures. A mass balance analysis of the products observed in GC is unable to account for all the material that reacts thereby implying the formation of non-volatile, higher M_w products, which are observed by GPC analysis. Fig. 7 shows the measured reactivity of EC as a function of temperature and different salts as determined by the rate of disappearance of the EC. It can be clearly seen that the solvent mixtures without Lewis acid salts are stable and that the most reactive salt is $LiPF_6$.

These observations may be rationalized according to the scheme shown in Fig. 8. Lewis acid-catalyzed ring-opening polymerization of EC (reaction (2), Fig. 8) is known but is an endothermic process at ambient temperatures [12,13]. The reaction is driven by the evolution of CO_2 from the oligo-ether carbonate polymer to yield PEO-like polymers (reaction (3), Fig. 8). Both the carbonate ethers and the PEO-like polymers can further react with PF_5. CO_2 gas is detected as the gaseous product from heated electrolyte solutions.

Within a well-sealed Li-ion cell, it is postulated that the evolution of CO_2 will cease once the solution is saturated. Consequently the polymerization of EC should also cease bringing the system to balance. Removal of the CO_2 should allow the polymerization to proceed and yield polymeric material that may deposit within the electrode structures and result in increased impedance and power fade. Fig. 9 shows the results of GPC analysis of aqueous extracts of 18650 anodes and cathodes that have undergone HEV testing at elevated temperatures (45 and 55 °C) for several weeks and have exhibited substantial power fade [10]. High M_w material is detected in all the electrode components examined.

CO_2 is reducible at the anode under normal conditions [14–16]. In a Li-ion battery, the reduction has to occur via electron transfer through the SEI layer and its is postulated

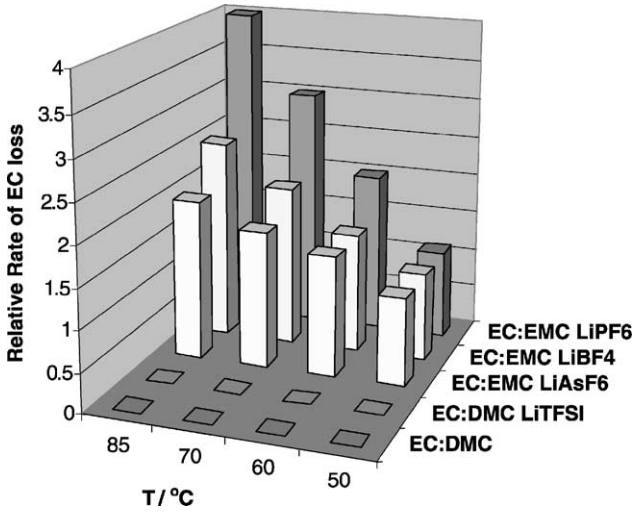

Fig. 7. Relative rates of EC loss with various salts. (1) EC:DMC solvent mixture is stable. (2) Solvent + LiTFSI salt is stable. (3) Solvent mixture is not stable with Lewis acid salts. (4) $LiPF_6$ appears most sensitive to heat.

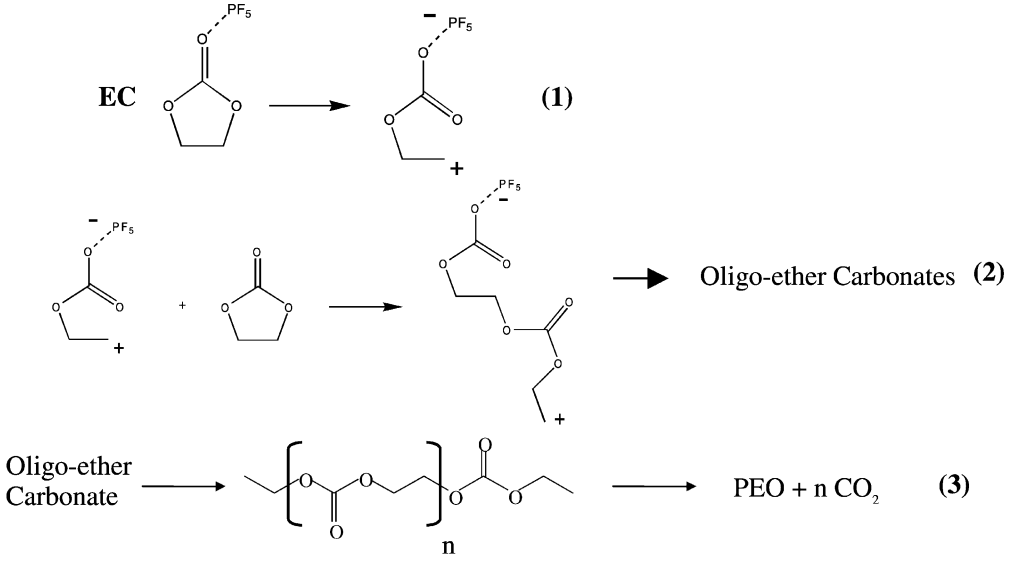

- **Gas (CO_2) is evolved after the electrolytes are heated.**
- **PEO reacts further with PF_5 and CO_2 is reduced to formate, oxalate, carbonate and CO**

Fig. 8. Acid-catalyzed ring-opening polymerization of EC accounts for observations. Note: reaction (2) is endothermic up to 170 °C.

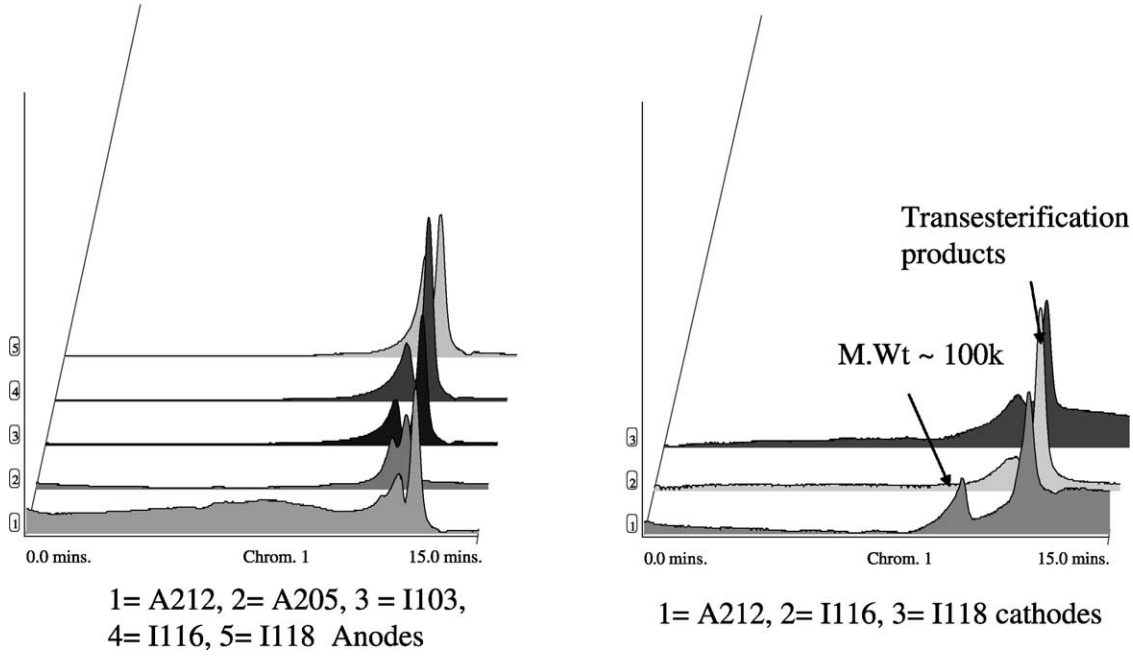

Fig. 9. Gel permeation chromatography (GPC) analysis of aqueous extracts of anodes (synthetic graphite) and cathodes ($LiAl_{0.05}Ni_{0.80}Co_{0.15}O_2$) from cycled and calendar life 18650 cells detects oligomer and polymer formation within the composite electrodes.

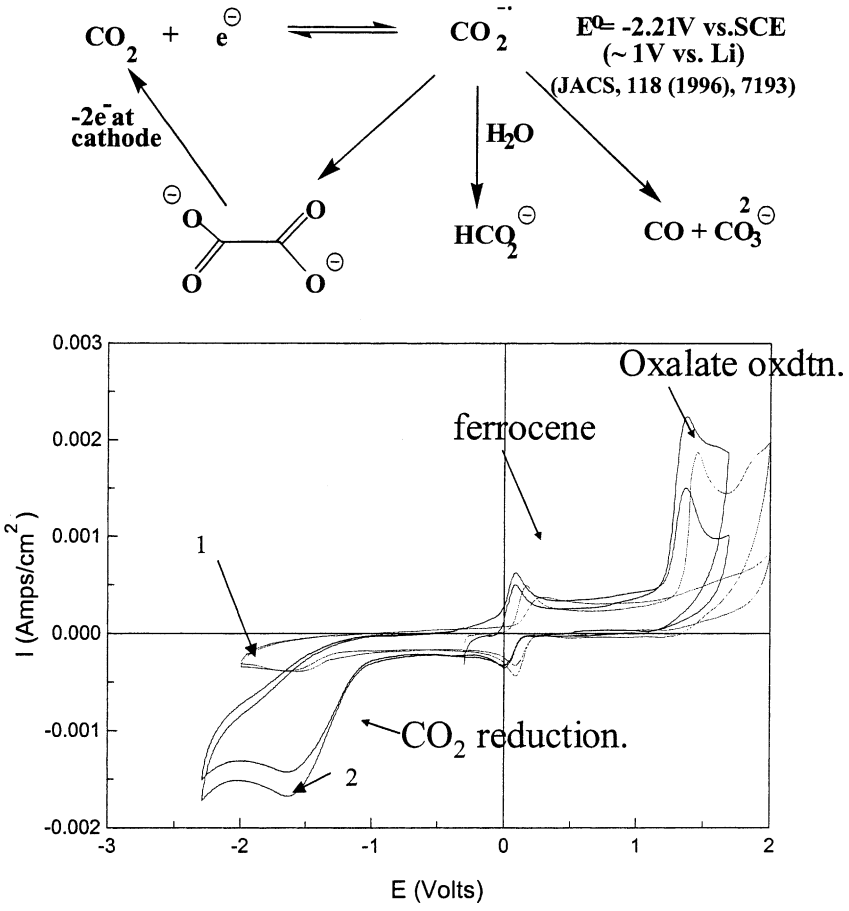

Fig. 10. Cyclic voltammetry demonstrates the CO_2 shuttle mechanism responsible for reversible self-discharge via oxalate formation. Formation of Li_2CO_3 and CO lead to irreversible capacity loss. Sodium oxalate (10 mM) at a glassy carbon electrode in EC/EMC 1 M $LiPF_6$. Reference is silver wire and ferrocene (5 mM); 50 mV/s sweep rate. Cycle 1 is carried out after solution flushed with argon. Cycle 2 carried out after prior cycling but no argon flush.

that CO_2 is more easily reduced than other components in the electrolyte [17]. Oxalate, carbonate formate and CO are formed by reduction of CO_2. Oxalate and formate can be re-oxidized at the cathode to CO_2 to give a reversible self-discharge mechanism (see Fig. 10). Reduction to CO and carbonate is an irreversible self-discharge mechanism that reduces capacity permanently and increases the SEI layer thickness on the anode. Removal of CO_2 from the solution by reduction at the anode or by some other means (e.g. leaking) allows more polymer formation which may result in power fade. CO_2 reduces to carbonate and CO on Cu in propylene carbonate and is known to produce CH_4 and other hydrocarbon gases on copper in the presence of water [18]. Although the production of methane and other hydrocarbon gases is well known during the formation cycle there is also a slow production of hydrocarbon gases during cycle and calendar life which corresponds with a decrease in CO_2 production. Slow reaction of CO_2 on exposed copper components is possible in addition to direct reduction of carbonate solvents on the anode. Fig. 10 shows the cyclic voltammogram of oxalate in carbonate solvents and the mechanism of CO_2 reduction that may operate. The oxidation potential for sodium oxalate is higher than normal Li-ion cell potentials but the voltammogram shows the ion-paired species. The oxidation potential of the non-ion-paired species will be considerably less and may be accessible at the long time scales of self-discharge through a pre-equilibrium CE mechanism [19].

4. Conclusions

The experiments described above unequivocally show that the typical electrolyte mixtures used in lithium-ion batteries are inherently unstable. This instability produces products that interact with the electrodes in beneficial and also undesirable ways. The beneficial reactions contribute to the formation and repair of the SEI layer which allows the battery to function while the undesirable reactions give rise to loss of capacity [20] and power [21]. The reactions investigated in this study and their consequences for battery operation are:

1. $LiPF_6$ acts as a Lewis acid with EC-containing solvents to generate transesterification products, PEO polymers and CO_2.
2. CO_2 is reduced at anodes to give oxalate, formate or carbonate and CO. The relative amounts depend on water content and current. Copper current collectors may yield hydrocarbon gases from CO_2 in the presence of trace water. Both carbon anodes and copper current collectors will be covered by passivating films through which the electrons must pass to the CO_2 and the other solvent components.
3. Oxalate may be re-oxidized to CO_2 to provide a reversible self-discharge mechanism.
4. CO_2 is reduced to lithium carbonate, CO and hydrocarbons in an irreversible self-discharge that reduce capacity.
5. Removal of CO_2 from solution allows further polymerization that leads to increased power fade and increased impedance.
6. Oxidation of PEO polymers above 3.6 V generates more acid and increases polymer formation to provide a state of charge dependence. The oxidation of benzyl ethers is known to take place at ~4 V versus Li [22] and may be catalyzed to occur at even lower potentials [23]. The oxidation of PEO-like material by this mechanism generates carbocations and protons that are capable of inducing polymerization or cross-linking reactions that lead to high M_w products in the composite cathode. This oxidation also rationalizes recent reports of facile oxidation of lithium-ion battery electrolytes [24].

These complex reactivity schemes are under study and more detailed descriptions will be provided in future publications. At this time the chemical reactivity described allows one to rationalize much observed behavior in lithium-ion batteries and is amenable to treatment with system models [25]. The reactions described here must surely play a role in the development and effectiveness of the SEI layer and are therefore of considerable interest for the understanding of the operation of Li-ion batteries. There is much scope for more detailed study of the chemistry of lithium-ion battery electrolytes to test the hypotheses presented in this paper.

Acknowledgements

This work was supported by the Assistant Secretary for Energy Efficiency and Renewable Energy, Office of FreedomCAR and Vehicle Technologies of the US Department of Energy under Contract No. DE-AC03-76SF00098. The authors would like to acknowledge the staff at Lawrence Berkeley National Laboratory, Argonne National Laboratory, Sandia National Laboratory, Idaho National Environmental Engineering Laboratory and Brookhaven National Laboratory, who contributed their results and valuable discussions from the U.S.DOE ATD program.

References

[1] G.E. Blomgren, J. Power Sources 82 (1999) 112.
[2] H. Kim, J. Choi, H.J. Sohn, T. Kang, J. Electrochem. Soc. 146 (1999) 4401.
[3] N.N. Greenwood, A. Earnshaw, Pergamon Press, New York, 1984, p. 1013.
[4] N.N. Greenwood, A. Earnshaw, Pergamon Press, New York, 1984, p. 572.
[5] K.O. Christe, D.A. Dixon, D. McLemore, W.W. Wilson, J.A. Sheehy, J.A. Boatz, J. Fluorine Chem. 101 (2000) 151.

[6] A.D. Holding, D. Pletcher, R.V.H. Jones, Electrochim. Acta 34 (1989) 1529.
[7] R.A. Wiesbock, US Patent 3,654,330 (1972).
[8] L.J. Krause, W. Lamanna, J. Summerfield, M. Engle, G. Korba, R. Loch, R. Atanasoski, J. Power Sources 68 (1997) 320.
[9] S.E. Sloop, J.K. Pugh, S. Wang, J.B. Kerr, K. Kinoshita, Electrochem. Solid State Lett. 4 (2001) A42.
[10] I. Bloom, B.W. Cole, J.J. Sohn, S.A. Jones, E.G. Polzin, V.S. Battaglia, G.L. Henriksen, C. Motloch, R. Richardson, T. Unkelhaeuser, D. Ingersoll, H.L. Case, J. Power Sources 101 (2001) 238.
[11] X. Zhang, P.N. Ross, R. Kostecki, F. Kong, S. Sloop, J.B. Kerr, K. Striebel, E.J. Cairns, F. McLarnon, J. Electrochem. Soc. 148 (2001) A463.
[12] L. Vogdanis, W. Heitz, Macromol. Chem., Rapid Commun. 7 (1986) 543.
[13] L. Vogdanis, B. Martens, H. Uchtmann, F. Hensel, W. Heitz, Makromol. Chem. Macromol. Chem. Phys. 191 (1990) 465.
[14] C. Amatore, J.M. Saveant, J. Am. Chem. Soc. 103 (1981) 5021.
[15] A. Gennaro, A.A. Isse, M.-G. Severin, E. Vianello, I. Bhugun, J.-M. Saveant, J. Chem. Soc., Faraday Trans. 92 (1996) 3963.
[16] A. Gennaro, A.A. Isse, J.-M. Saveant, M.-G. Severin, E. Vianello, J. Am. Chem. Soc. 118 (1996) 7190.
[17] S. Ikeda, T. Takagi, K. Ito, Bull. Chem. Soc. Jpn. 60 (1987) 2517.
[18] R.L. Cook, R.C. MacDuff, A.F. Sammells, J. Electrochem. Soc. 135 (1988) 1320.
[19] J.M. Saveant, J. Phys. Chem. B 105 (2001) 8995.
[20] M. Broussely, S. Herreyre, P. Biensan, P. Kasztejna, K. Nechev, R.J. Staniewicz, J. Power Sources 97 (8) (2001) 13.
[21] K. Amine, C.H. Chen, J. Liu, M. Hammond, A. Jansen, D. Dees, I. Bloom, D. Vissers, G. Henriksen, J. Power Sources 97 (8) (2001) 684.
[22] J.W. Boyd, P. Schmazl, L.L. Miller, J. Am. Chem. Soc. 102 (1980) 3856.
[23] W. Schmidt, E. Steckhan, Angew. Chem. 91 (1979) 850.
[24] M. Moshkovich, M. Cojocaru, H.E. Gottlieb, D. Aurbach, J. Electroanal. Chem. 497 (2001) 84.
[25] P. Arora, R.E. White, M. Doyle, J. Electrochem. Soc. 145 (1998) 3647.